Destruction of the cosmic γ-ray emitter 26Al in massive stars: Study of the key 26Al(n,p) reaction

(n_TOF Collaboration) Lederer-Woods, C.; Woods, P. J.; Davinson, T.; Kahl, D.; Lonsdale, S. J.; Aberle, O.; Amaducci, S.; Andrzejewski, J.; Audouin, L.; Bacak, M.; ...

Destruction of the cosmic γ-ray emitter ^{26}Al in massive stars: Study of the key ^{26}Al(n, p) reaction

C. Lederer-Woods,[1,*] P. J. Woods,[1] T. Davinson,[1] D. Kahl,[1,†] S. J. Lonsdale,[1] O. Aberle,[2] S. Amaducci,[3,4] J. Andrzejewski,[5]
L. Audouin,[6] M. Bacak,[7,2,8] J. Balibrea,[9] M. Barbagallo,[10] F. Bečvář,[11] E. Berthoumieux,[8] J. Billowes,[12] D. Bosnar,[13]
A. Brown,[14] M. Caamaño,[15] F. Calviño,[16] M. Calviani,[2] D. Cano-Ott,[9] R. Cardella,[2] A. Casanovas,[16] F. Cerutti,[2] Y. H. Chen,[6]
E. Chiaveri,[2,12,17] N. Colonna,[10] G. Cortés,[16] M. A. Cortés-Giraldo,[17] L. Cosentino,[18] S. Cristallo,[19,20] L. A. Damone,[10,21]
M. Diakaki,[8] C. Domingo-Pardo,[22] R. Dressler,[23] E. Dupont,[8] I. Durán,[15] B. Fernández-Domínguez,[15] A. Ferrari,[2]
P. Ferreira,[24] F. J. Ferrer,[25] P. Finocchiaro,[18] V. Furman,[26] K. Göbel,[27] A. R. García,[9] A. Gawlik,[5] S. Gilardoni,[2] T. Glodariu,[28]
I. F. Gonçalves,[24] E. González-Romero,[9] E. Griesmayer,[7] C. Guerrero,[17] F. Gunsing,[8,2] H. Harada,[29] S. Heinitz,[23] J. Heyse,[30]
D. G. Jenkins,[14] E. Jericha,[7] F. Käppeler,[31] Y. Kadi,[2] A. Kalamara,[32] P. Kavrigin,[7] A. Kimura,[29] N. Kivel,[23] M. Kokkoris,[32]
M. Krtička,[11] D. Kurtulgil,[27] E. Leal-Cidoncha,[15] H. Leeb,[7] J. Lerendegui-Marco,[17] J. Lo Meo,[33,3] D. Macina,[2] A. Manna,[3,4]
J. Marganiec,[5,34] T. Martínez,[9] A. Masi,[2] C. Massimi,[3,4] P. Mastinu,[35] M. Mastromarco,[10] E. A. Maugeri,[23] A. Mazzone,[10,36]
E. Mendoza,[9] A. Mengoni,[33] P. M. Milazzo,[37] F. Mingrone,[2] A. Musumarra,[18,38] A. Negret,[28] R. Nolte,[34] A. Oprea,[28]
N. Patronis,[39] A. Pavlik,[40] J. Perkowski,[5] I. Porras,[41] J. Praena,[41] J. M. Quesada,[17] D. Radeck,[34] T. Rauscher,[42,43] R. Reifarth,[27]
C. Rubbia,[2] J. A. Ryan,[12] M. Sabaté-Gilarte,[2,17] A. Saxena,[44] P. Schillebeeckx,[30] D. Schumann,[23] P. Sedyshev,[26] A. G. Smith,[12]
N. V. Sosnin,[12] A. Stamatopoulos,[32] G. Tagliente,[10] J. L. Tain,[22] A. Tarifeño-Saldivia,[16] L. Tassan-Got,[6] S. Valenta,[11]
G. Vannini,[3,4] V. Variale,[10] P. Vaz,[24] A. Ventura,[3] V. Vlachoudis,[2] R. Vlastou,[32] A. Wallner,[45] S. Warren,[12] C. Weiss,[7]
T. Wright,[12] and P. Žugec[13,2]

(n_TOF Collaboration)

[1]*School of Physics and Astronomy, University of Edinburgh, Peter Guthrie Tait Road, EH9 3FD Edinburgh, United Kingdom*
[2]*European Organization for Nuclear Research (CERN), Switzerland*
[3]*Istituto Nazionale di Fisica Nucleare, Sezione di Bologna, Italy*
[4]*Dipartimento di Fisica e Astronomia, Università di Bologna, Italy*
[5]*University of Lodz, Poland*
[6]*Institut de Physique Nucléaire, CNRS-IN2P3, Univ. Paris-Sud, Université Paris-Saclay, F-91406 Orsay Cedex, France*
[7]*Technische Universität Wien, Austria*
[8]*CEA Irfu, Université Paris-Saclay, F-91191 Gif-sur-Yvette, France*
[9]*Centro de Investigaciones Energéticas Medioambientales y Tecnológicas (CIEMAT), Spain*
[10]*Istituto Nazionale di Fisica Nucleare, Sezione di Bari, Italy*
[11]*Charles University, Prague, Czech Republic*
[12]*University of Manchester, United Kingdom*
[13]*Department of Physics, Faculty of Science, University of Zagreb, Zagreb, Croatia*
[14]*University of York, United Kingdom*
[15]*University of Santiago de Compostela, Spain*
[16]*Universitat Politècnica de Catalunya, Spain*
[17]*Universidad de Sevilla, Spain*
[18]*INFN Laboratori Nazionali del Sud, Catania, Italy*
[19]*Istituto Nazionale di Fisica Nucleare, Sezione di Perugia, Italy*
[20]*Istituto nazionale di Astrofisica - Osservatorio Astronomico d'Abruzzo, Italy*
[21]*Dipartimento di Fisica, Università degli Studi di Bari, Italy*
[22]*Instituto de Física Corpuscular, CSIC - Universidad de Valencia, Spain*
[23]*Paul Scherrer Institut (PSI), Villingen, Switzerland*
[24]*Instituto Superior Técnico, Lisbon, Portugal*
[25]*Centro Nacional de Aceleradores (U. Sevilla, J. Andalucia, CSIC), Spain*
[26]*Joint Institute for Nuclear Research (JINR), Dubna, Russia*
[27]*Goethe University Frankfurt, Germany*
[28]*Horia Hulubei National Institute of Physics and Nuclear Engineering, Romania*
[29]*Japan Atomic Energy Agency (JAEA), Tokai-mura, Japan*
[30]*European Commission, Joint Research Centre, Geel, Retieseweg 111, B-2440 Geel, Belgium*

*claudia.lederer-woods@ed.ac.uk

†Present address: Extreme Light Infrastructure - Nuclear Physics, Horia Hulubei National Institute for R&D in Physics and Nuclear Engineering (IFIN-HH), 077125 Bucharest-Magurele, Romani.

^{31}*Karlsruhe Institute of Technology, Campus North, IKP, 76021 Karlsruhe, Germany*
^{32}*National Technical University of Athens, Greece*
^{33}*Agenzia nazionale per le nuove tecnologie (ENEA), Bologna, Italy*
^{34}*Physikalisch-Technische Bundesanstalt (PTB), Bundesallee 100, 38116 Braunschweig, Germany*
^{35}*Istituto Nazionale di Fisica Nucleare, Sezione di Legnaro, Italy*
^{36}*Consiglio Nazionale delle Ricerche, Bari, Italy*
^{37}*Istituto Nazionale di Fisica Nucleare, Sezione di Trieste, Italy*
^{38}*Dipartimento di Fisica e Astronomia, Università di Catania, Italy*
^{39}*University of Ioannina, Greece*
^{40}*University of Vienna, Faculty of Physics, Vienna, Austria*
^{41}*University of Granada, Spain*
^{42}*Department of Physics, University of Basel, Switzerland*
^{43}*Centre for Astrophysics Research, University of Hertfordshire, United Kingdom*
^{44}*Bhabha Atomic Research Centre (BARC), India*
^{45}*Australian National University, Canberra, Australia*

The ^{26}Al(n, p) ^{26}Mg reaction is the key reaction impacting on the abundances of the cosmic γ-ray emitter ^{26}Al produced in massive stars and impacts on the potential pollution of the early solar system with ^{26}Al by asymptotic giant branch stars. We performed a measurement of the ^{26}Al(n, p) ^{26}Mg cross section at the high-flux beam line EAR-2 at the n_TOF facility (CERN). We report resonance strengths for eleven resonances, nine being measured for the first time, while there is only one previous measurement for the other two. Our resonance strengths are significantly lower than the only previous values available. Our cross-section data range to 150 keV neutron energy, which is sufficient for a reliable determination of astrophysical reactivities up to 0.5 GK stellar temperature.

The long-lived radioisotope ^{26}Al ($T_{1/2} = 0.7$ Myr) plays a unique role for our understanding of the origin of the chemical elements in the cosmos. Its presence can be directly observed in our galaxy by its decay radiation [1], providing proof of ongoing nucleosynthesis, and giving clues about nucleosynthesis processes inside stars.

Identifying the astrophysical sites and stellar yields of ^{26}Al provides important information to study galactical chemical evolution, supernova explosions, and may help to understand the formation of our solar system (extinct ^{26}Al found in meteorites suggests that ^{26}Al was injected into the solar system just before its formation [2]).

Significant progress to identify the origin of galactic ^{26}Al has been made by detailed satellite observations of its abundance distribution across the galaxy (COMPTEL [3] and INTEGRAL [4]), suggesting massive stars as most likely sites for ^{26}Al production. Stellar models link ^{26}Al production to three distinct stellar sites in massive stars [5–7]: (i) the hydrogen-burning phase in Wolf Rayet stars [8], (ii) convective C burning, and (iii) explosive Ne/C burning in stars before and during core collapse. A missing piece of information is the experimental determination of nuclear reaction rates which influence the amount of ^{26}Al produced in these different stellar sites. Major uncertainties to determine ^{26}Al abundances in sites (ii) and (iii) are the neutron-induced destruction reactions (n, α) and (n, p). In their sensitivity study, Iliadis *et al.* [6] conclude that present uncertainties of the ^{26}Al(n, p) reaction at stellar temperatures above 1 GK have the most impact on estimates of overall ^{26}Al production in massive stars.

Among the candidates for the pollution of the early solar system with ^{26}Al are asymptotic giant branch (AGB) stars [9]. The contribution of low-mass (<4 M$_\odot$) AGB stars to this process depends sensitively on how much ^{26}Al is destroyed by the neutron-induced (n, p) and (n, α) reactions. This requires an accurate knowledge of these reaction rates for stellar temperatures around 0.3 GK.

Experimental data on ^{26}Al(n, p) reaction cross sections are scarce, with only two direct measurements [10,11], and results from these measurements are highly discrepant in the energy range of overlap (see Ref. [6] for discussion). The first direct measurement of the ^{26}Al(n, p) cross sections was performed by Trautvetter *et al.* [11], who measured averaged cross sections using four different neutron spectra with average energies of 40 meV, 30 keV, 70 keV, and 300 keV. In particular, the neutron spectra with energies of 30 and 70 keV were similar in shape to Maxwell Boltzmann distributions, which allowed Trautvetter *et al.* to directly infer the astrophysical reaction rate. Trautvetter *et al.* also provided branchings for proton emission to the ground (n, p_0), first (n, p_1), and, in the thermal case, second (n, p_2) excited state of ^{26}Mg. They concluded that the reaction rate is dominated by the (n, p_1) channel. The second and only subsequent direct measurement was performed by Koehler *et al.* [10] using the neutron time-of-flight technique at the LANSCE facility at Los Alamos National Laboratory. They measured energy-dependent ^{26}Al(n, p_1) cross sections up to 70 keV, identifying two resonances, one at 5.6 keV neutron energy, and one around 35 keV neutron energy. Their data were normalized to the thermal ^{26}Al(n, p_1) cross section determined by Trautvet-

ter *et al.* [11]. Despite normalizing to the value of Trautvetter *et al.* at lower energy, it turned out that astrophysical reactivities calculated using the Koehler *et al.* data were significantly higher than those derived with the data of Trautvetter *et al.* (see, e.g., Refs. [6,12] for a discussion). It should be noted that the most recent study identifying states in ^{27}Al above the neutron separation energy, performed via the ^{27}Al(p, p') reaction by Benamara *et al.* [13], indicate about 7–8 states per 100 keV. This is similar to results by de Smet *et al.*'s [14] study of the ^{26}Al(n, α) channel, where six resonances were observed below neutron energies of 110 keV, suggesting that the ^{26}Al(n, p) cross section may be strongly influenced by several resonances not observed yet. Therefore, new data on this important reaction are urgently required to resolve the discrepancies between existing experimental data.

We simultaneously measured ^{26}Al(n, p) and ^{26}Al(n, α) reaction cross sections at the neutron time-of-flight facility n_TOF at CERN. This paper reports on results for the ^{26}Al(n, p) reaction; results on the ^{26}Al(n, α) reaction will be published in a subsequent article [15].

At n_TOF, a highly intense pulsed neutron beam is produced by spallation reactions of a 20-GeV proton beam impinging on a massive Pb target. The initially highly energetic neutrons are slowed down by using a water moderator surrounding the target. This results in a neutron spectrum ranging from thermal-neutron energies (25 meV) to several GeV. The measurement was performed at the recently commissioned vertical high-flux beam line EAR-2 at a distance of about 20 m from the spallation target [16]. We used a large neutron beam collimator with a diameter of 8.6 cm to maximize the neutron flux. This allowed us to achieve good statistical accuracy despite the small sample mass due to ^{26}Al being radioactive. The ^{26}Al sample was produced by Los Alamos National Laboratory and EC-JRC Geel about 20 years ago [17]. It has an active area of 5×6 cm^2 and consists of $2.58(12) \times 10^{17}$ atoms ^{26}Al [14,17].

The (n, p) reaction cross section on ^{26}Al was measured by using a silicon strip detection setup housed in an aluminium reaction chamber (see Fig. 1). The detection setup consisted of two 50×50 mm^2 silicon strip detectors, arranged as a ΔE-E telescope. The ΔE detector was a 20-μm-thick single-sided silicon strip detector (SSD, 16 strips). Placed behind it was a 50 μm SSD (16 strips). Proton energies for the main reaction channels are about 4.6 MeV for ^{26}Al(n, p_0) events, about 2.9 MeV for ^{26}Al(n, p_1), and 1.8 MeV for ^{26}Al(n, p_2). In all those cases, protons will produce a signal above threshold both in the ΔE and the E detectors (a 1 MeV proton has a range of ≈ 20 μm in silicon). In contrast, events produced in the ^{26}Al(n, α) reaction can be eliminated because they are stopped already in the thin 20 μm ΔE detector. Protons emitted by the (n, p_2) branch are completely stopped in the ΔE-E system, while protons of the (n, p_1) branch are only stopped if emitted at certain angles (the range of 2.9 MeV protons in silicon is about 90 μm, so slightly larger than the combined $20 + 50$ μm thickness of the SSDs), and protons from the (n, p_0) channel are not stopped. A thicker E detector, which would stop all protons, was not chosen because the γ flash (highly intense, prompt γ radiation produced when the proton pulse hits the spallation target) was found to saturate
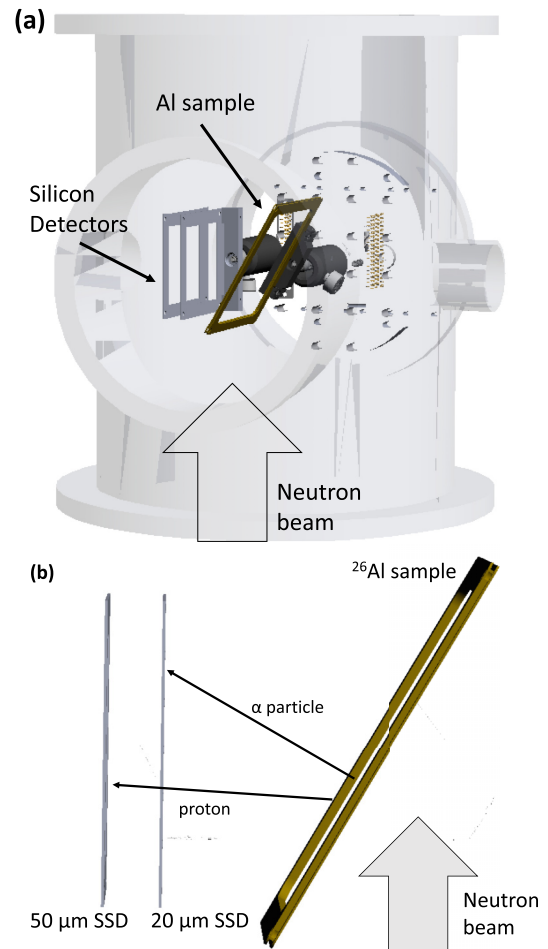

FIG. 1. (a) Reaction chamber with silicon detectors and Al sample. (b) ΔE-E telescope setup to identify protons emitted in ^{26}Al(n, p) reactions.

thicker detectors, which would have had the effect of lowering the upper neutron energy limit. Data were recorded using flash ADCs (12 and 14 bit at sampling rates of 56.25 and 62.5 MHz, respectively). We developed a dedicated pulse shape analysis algorithm for the present experimental setup to analyze signals as close as possible to the γ flash. This allowed us to reach an upper neutron energy limit of 150 keV, the highest energy reached so far in a time-of-flight measurement of the ^{26}Al(n, p) reaction.

The detection efficiency of the setup was determined by normalizing the data to the well-known ^{10}B(n, α) cross section between 1 and 100 eV [18], using a ^{10}B sample of the same size as the ^{26}Al sample. The thickness of this ^{10}B sample has been determined with an accuracy of 5% by a proton-elastic backscattering spectrometry measurement performed at the 3 MV tandem pelletron accelerator at the Centro Nacional de Aceleradores (CNA, Spain). The different neutron fluences on the Al and B samples were measured by recording the number of protons hitting the spallation target (which is proportional to the number of neutrons produced). An uncertainty of 3% for this fluence normalization was determined by monitoring the stability of the number of counts in the silicon
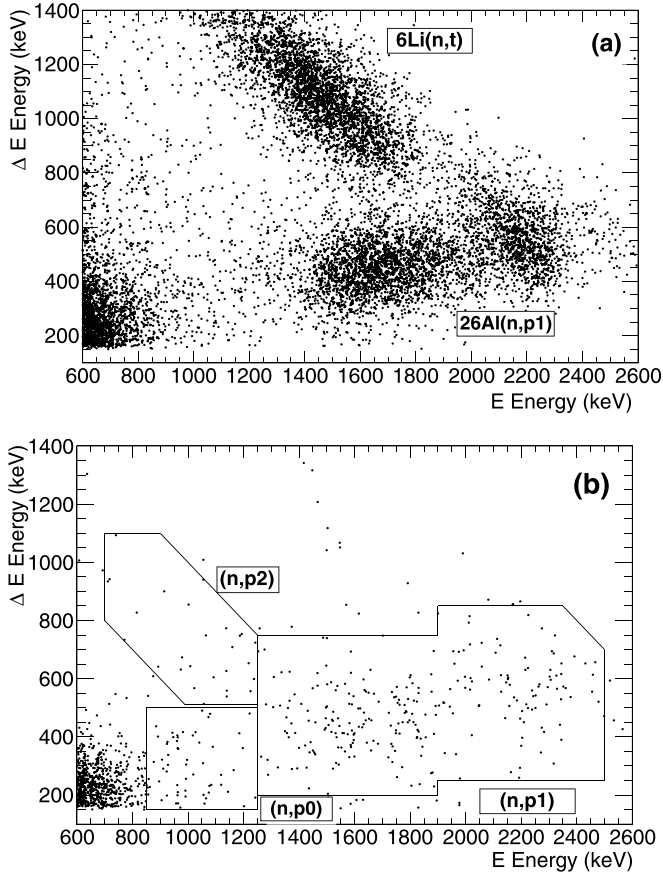
FIG. 2. (a) ΔE vs E energy across the entire neutron energy range from thermal (25 meV) to 150 keV. Clear groups of events can be observed for ^{26}Al(n, p_1) and ^{6}Li(n, t) reactions. ^{26}Al(n, p_1) events are spread over two groups as some protons do not get stopped in the ΔE-E system. (b) Same as (a) but for events corresponding to neutron energies in the resonance region (1–150 keV).

detectors normalized to the protons on target for each run. The uncertainty of the ^{10}B(n, α) cross section used as a reference is negligible compared with the other systematic uncertainties ($<1\%$) [18]. Alpha particles emitted in the ^{10}B(n, α) reaction are already stopped in the ΔE detector. To take into account the difference in efficiency compared with proton detection, which requires a coincidence between ΔE and the E detector at a larger distance to the sample, we also measured ^{6}Li(n, t) reactions using a LiF sample enriched in ^{6}Li. Using the ratio of tritons detected in ΔE and tritons detected in coincidence between the ΔE and E detectors, we determined the proton detection efficiency relative to the α detection efficiency of $\epsilon_p/\epsilon_\alpha = 0.70(4)$.

Figure 2(a) shows ΔE vs E detector energies of ^{26}Al sample data across the entire neutron energy range. Most of the events are associated with the high yield for reactions induced by thermal neutrons (see Fig. 3). The ^{26}Al(n, p_1) events are split across two groups, since a fraction of the protons are not completely stopped in the E detector. There is another group from tritons produced by the ^{6}Li(n, t) reaction due to a small ^{6}Li impurity in the sample or reaction chamber. Figure 2(b) is restricted to events gated on neutron energies in the reso-
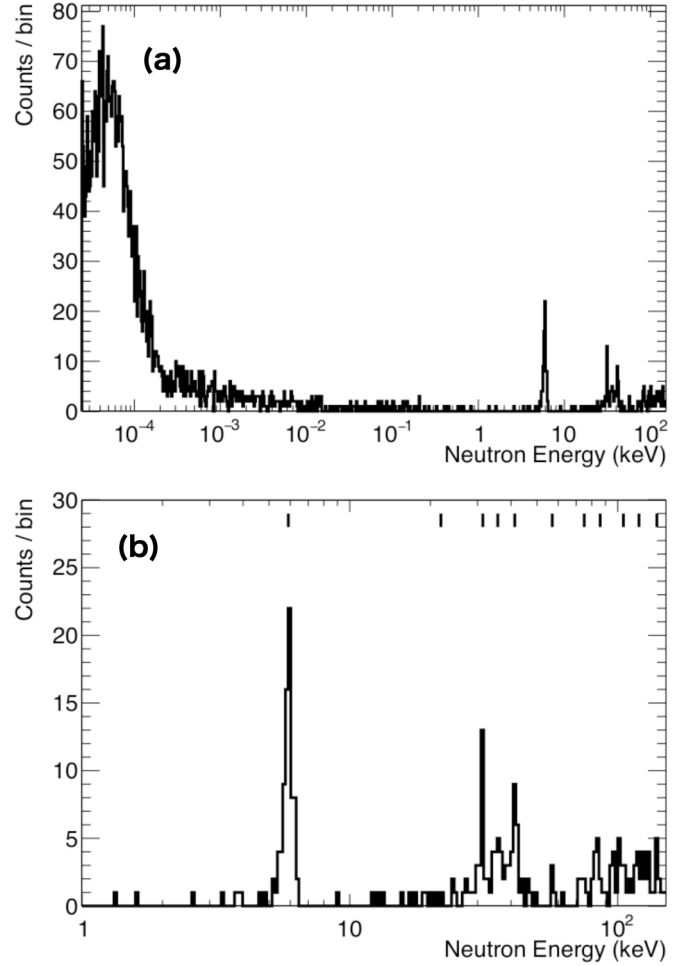

FIG. 3. (a) ^{26}Al(n, p_1) count spectrum over the whole neutron energy range from thermal (2.5×10^{-5} keV) to 150 keV. (b) Zoom into the resonance region. The positions of present and previously observed resonances are marked by black lines and listed in Table I.

TABLE I. Resonance energies and resonance strengths $\omega\gamma$ of the ^{26}Al(n, p_1) reaction compared with previous data by Koehler *et al.* [10]. The quoted uncertainties are only due to propagating uncorrelated uncertainties due to counting statistics. The combined uncertainties due to systematic effects are 10%.

This work		Koehler *et al.* [10]	
E_R (keV)	$\omega\gamma_{p1}$ (eV)	E_R (keV)	$\omega\gamma_{p1}$ (eV)
5.9(1)	1.28(16)	5.578	2.03(51)
21.9(2)	<0.6		
31.4(4)	5.8(14)		
35.7(4)	43.4(98)	33.7	128(22)
41.3(4)	22.9(48)		
57(2)	2.7(18)		
75(2)	8.1(36)		
86(4)	85(21)		
≈105	53(13)		
≈120	46(12)		
≈140	71(22)		

nance region from 1 to 150 keV (see Fig. 3). Events from the ^{6}Li(n, t) reaction completely disappear as they are dominantly produced by thermal neutrons. The regions of interest for the ^{26}Al(n, p_0) and ^{26}Al(n, p_2) channels are also shown along with the dominant (n, p_1) grouping. For the ^{26}Al(n, p_0) events a more restricted region has been selected corresponding to a minimum E signal energy of 850 keV due to background noise in the energy region below. This results in a loss of about 20% of ^{26}Al(n, p_0) events.

Figures 3(a) and 3(b) show the neutron energy spectrum for the dominant ^{26}Al(n, p_1) channel including the thermal-neutron-induced events and for the resonance region, respectively, gating on ΔE and E energies of ^{26}Al(n, p_1) events shown in Fig. 2. Table I shows a list of the resonance energies and strengths from the present work compared with those seen in the earlier work of Kohler *et al.* [10]. The data from the energy spectrum was first converted to a cross section using $\sigma = C_{Al}/(\epsilon n_{Al}\Phi)$ where C_{Al} is the proton count rate, n_{Al} is the areal density of the sample, ϵ is the detection efficiency and Φ is the neutron fluence rate (determined in a separate campaign [19]). Resonance strengths were then calculated using $\omega\gamma = Ak^2/(2\pi^2)$, where A is the resonance area (eV barn) and k is the wave number. Potential background caused by beam induced reactions was estimated for each resonance by considering counts in regions outside the resonances, which produced small changes (3%–15%) in the calculated resonance strengths (see Fig. 3). In a run with no neutron beam (1/8 duration compared with ^{26}Al sample run) there were no background events. The individual resonance strength uncertainties listed in Table I are only due to counting statistics. Uncertainties due to systematic effects are 10%, due to the energy distribution of the neutron fluence rate (2.7%) [19], the Al sample areal density (5%) [14,17], the B reference sample areal density (5%), the fluence normalization (3%), and the efficiency for coincident detection (6%), added in quadrature. An upper limit at a 95% confidence level on the strength is given in Table I for a resonance at 21.9 keV, which has only been previously observed in the (n, α) channel [14].

Only two resonance strengths were reported in the ^{26}Al(n, p_1) reaction measurement by Koehler *et al.* [10]. The resonance strength at 5.9 keV measured here is about a factor 1.5 weaker than in Ref. [10]. The second resonance reported in Ref. [10] is at 33.7 keV with a strength of 128 eV. In the data of Ref. [10], one broad resonance is shown at this neutron energy, suggesting that this resonance strength should probably be compared with the sum of three resonance strengths in this work (31.4, 35.7, and 41.3 keV). Taking this approach, our total strength in this region yields $72 \pm 11_{\text{stat}} \pm 7_{\text{sys}}$ eV, still almost a factor of two smaller than Ref. [10]. All resonances in the table below 110 keV except for $E_R = 31.4, 57$ and 75 keV have also been observed previously in the (n, α) channel [14]. For the energy region above 100 keV, we find indications for several resonances, but the experimental resolution precludes us from assigning precise resonance energies. Therefore, we provide resonance strengths for these resonance energies, integrating from 95–115, 115–130, and 130–150 keV, respectively. Previous data by Benamara *et al.* [13] where excitation energies above the neutron separation energy in ^{27}Al were identified using ^{27}Al$(p, p')^{27}$Al* reactions, quote states cor-

responding to about 110, 125, and 140 keV neutron energy, which is largely consistent with our data considering their excitation energy uncertainties of 4 keV [13].

We determined the ^{26}Al(n, p_1) cross section at thermal-neutron energies (25 meV) of 2519(247) mb. This can be compared with previous measurements performed by Trautvetter *et al.* and Wagemans *et al.* [11,20]. In both latter cases, the cross section has been determined in a Maxwellian spectrum of a thermal reactor while in our case we provide a pointwise rather than averaged cross section. Our Maxwellian-averaged cross section at $kT = 40$ meV is 1960(198) mb, in agreement with Trautvetter *et al.*'s value of 1850(150) mb. At $kT = 36$ meV, corresponding to Wagemans *et al.*'s neutron spectrum, we obtain 2065(210) mb, again in good agreement to Wagemans *et al.*'s value of 1942(95) mb.

For the reaction channel to the ground state of ^{26}Mg, (n, p_0), we obtain strengths for individual resonances; at 86 keV of 43(18) eV, and at around 140 keV of 51(22) eV. For the ^{26}Al(n, p_2) channel, the statistics in individual resonances were not high enough to extract meaningful information, however, astrophysical reaction rates could be obtained for this channel (see below).

We have calculated astrophysical reactivities $N_A\langle\sigma v\rangle$ for all three branches (N_A is the Avogadro number). For the ^{26}Al(n, p_0) and ^{26}Al(n, p_1) channels, where we could extract reliable resonance information below 95 keV, we have used the approach by Macklin and Gibbons [21], i.e.,

$$\langle\sigma v\rangle = \left(\frac{2k_BT}{\mu}\right)^{1/2} \sigma_{\text{th}} \left(\frac{25.3 \times 10^{-6} \text{ [keV]}}{k_BT \text{ [keV]}}\right)^{1/2}$$
$$+ \left(\frac{2\pi}{\mu k_BT}\right)^{3/2} \hbar^2 \Sigma_i \omega\gamma(i) \exp^{-E_R(i)/k_BT}. \quad (1)$$

This was complemented by using the experimental cross-section information between 95 and 150 keV, i.e.,

$$\langle\sigma v\rangle = \left(\frac{8}{\pi\mu}\right)^{1/2} \frac{1}{(k_BT)^{3/2}} \int \sigma(E)E \exp^{-E/k_BT} dE. \quad (2)$$

Here μ is the reduced mass, k_B is the Boltzmann constant, and T is the stellar temperature. σ_{th} is the cross section at the thermal-neutron energy (25 meV), and this term accounts for its contribution to the rate, using the well-known $1/v$ energy dependence of the reaction cross section at low neutron energy. For the ^{26}Al(n, p_2) channel, the reactivity was calculated using Eq. (2) over the whole energy range. Backgrounds affecting the average cross section $\sigma(E)$ used in Eq. (2) were estimated again by considering events between resonances. For ^{26}Al(n, p_0) and ^{26}Al(n, p_1), a background between 95 and 150 keV of 20% and 5%, respectively, was estimated by using the resonance-free neutron energy region from 60 to 70 keV (above that, resonances are too closely spaced to estimate a background). For ^{26}Al(n, p_2) where the reactivity was determined using Eq. (2) over the whole range, the background was estimated in the resonance-free regions below 95 keV, which resulted in a correction of about 20%.

Figure 4 shows the reactivity $N_A\langle\sigma v\rangle$ up to 5 GK stellar temperature compared with other experimental data and
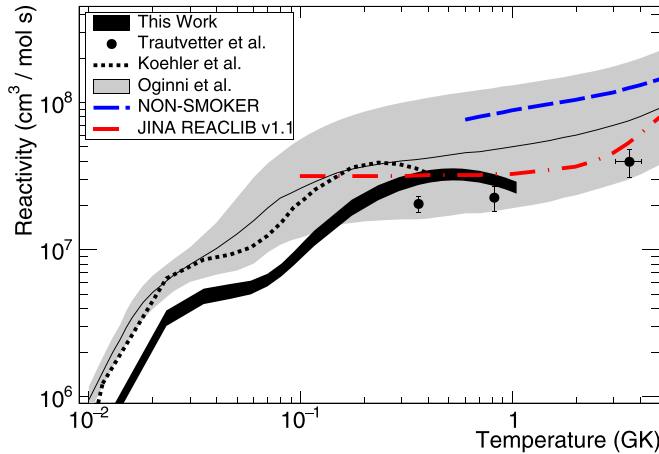
FIG. 4. Stellar reaction rate compared with previous measurements by Trautvetter *et al.* [11], Koehler *et al.* [10], and theoretical calculations and evaluations [12,22,23].

TABLE II. Reactivities of this work compared with those of Trautvetter *et al.* [11].

T (GK)		Reactivity $N_A \langle \sigma v \rangle$ (10^6 cm^3 mol^{-1} s^{-1})	
		This work	Trautvetter *et al.*
0.36	p_0	3.0(10)	1.9(9)
0.36	p_1	26.2(39)	18.6(25)
0.36	p_2	1.5(6)	
0.82	p_0	5.0(15)	3.6(29)
0.82	p_1	23.1(32)	19.0(32)
0.82	p_2	1.7(7)	
≈ 3.6	p_0		8.6(39)
≈ 3.6	p_1		30.1(78)

theoretical predictions. Our total ^{26}Al(n, p) rates are shown as the black band. Our data are reliable up to 0.5–0.6 GK. Above these temperatures, cross sections above our experimental range increasingly contribute to the total reactivity, meaning that our data provide a lower limit. The large error band in the recommended reactivity by Oginni *et al.* [12] reflects the discrepancies between experimental data by Trautvetter *et al.* [11], Koehler *et al.* [10], and theoretical calculations of the reactivity. Up to temperatures of 0.1 GK, our reactivity is smaller than even the low-energy limit suggested by Oginni *et al.*, and significantly smaller than rates by Koehler *et al.* Compared with Trautvetter *et al.*, our results are systematically higher. The figure also includes theoretical predictions and recommended values of the reactivity by NON-SMOKER [22], and JINA-REACLIB v1.1 [23] (which adopts rates by Caughlan and Fowler [24]), both based on Hauser-Feshbach calculations. It should be noted that statistical model predictions become unreliable at low level densities, as not enough resonances contribute to the overall reactivity (Ref. [22] estimates that this is the case for the ^{26}Al(n, p) reaction for stellar temperatures lower than 0.5–0.6 GK). Hence, a comparison with the experimental data is of limited significance.

Table II compares $N_A \langle \sigma v \rangle$ with results from Trautvetter *et al.* [11]. At 0.36 GK, both the (n, p_0) and (n, p_1) rates are higher but consistent within 1 and 2 standard deviations, respectively. In addition, our results suggest that about 5% of the total rate comes from (n, p_2) reactions which have not been published by Trautvetter *et al.* The agreement seems better at 0.82 GK, however, as mentioned before, our rates are likely underestimated due to the 150 keV neutron energy limit in our data. Compared with the median rate recommended by Oginni *et al.* [12] for ^{26}Al(n, p), our rate is about a factor of 2.5 smaller at 0.1 GK, while at 0.6 GK our rate is a factor of about 1.4 smaller.

The new reactivities represent an important input to model ^{26}Al destruction in AGB stars to investigate their role in the early solar system. For example, Ref. [25] finds that scaling

all neutron induced rates on ^{26}Al by a factor two reduces the amount of ^{26}Al by half, indicating that ^{26}Al produced in AGB stars is highly sensitive to neutron-induced reaction rates [in particular (n, p) and (n, α) because the (n, γ) rate is much smaller]. Regarding massive stars, the reasonable agreement of our results with those of Trautvetter *et al.* [11] at 0.36 GK indicates that Trautvetter *et al.*'s data at the higher stellar temperatures are a reasonable choice to use in stellar models.

In summary, we have measured ^{26}Al(n, p) reactions over a wide energy range at the high-flux beam line EAR-2 at n_TOF (CERN) using a dedicated silicon strip detection system. We obtain resonance energies and strengths of 11 resonances, with systematic uncertainties of 10%. Astrophysical reactivities were calculated including all relevant branches (n, p_0), (n, p_1), and (n, p_2), and are significantly lower than Koehler *et al.* in the energy range of overlap [10], and slightly higher than activation data from Trautvetter *et al.* [11]. Our results significantly constrain reaction-rate uncertainties compared with the current recommended rate uncertainties by Oginni *et al.* [12], providing accurate reactivities up to 0.5 GK and an improved lower limit of the reaction rate for higher stellar temperatures up to 1 GK. Our reasonable agreement with Trautvetter *et al.* for overlapping temperature ranges suggest that Trautvetter *et al.*'s rates at higher stellar temperatures (>1 GK) are presently a reasonable choice for stellar models. However, in the future, a measurement of this key reaction rate at higher neutron energies is very important to further constrain the reaction rate at the higher stellar temperatures (>1 GK) relevant for ^{26}Al destruction in massive stars.

[1] W. Mahoney, J. C. Ling, A. S. Jacobson, and R. E. Lingenfelter, Astrophys. J. **262**, 742 (1982).

[2] K. D. McKeegan and A. M. Davies, in *Treatise on Geochemistry Vol. 1: Meteorites, Comets and Planets*, edited by H. D. Holland and K. K. Turekian, 2nd edition (Elsevier, Oxford, 2007).

[3] J. Knödlseder, Astrophys. J. **510**, 915 (1999).

[4] R. Diehl, H. Halloin, K. Kretschmer, G. G. Lichti, V. Schönfelder, A. W. Strong, A. Kienlin, W. Wang, P. Jean, J. Knödlseder *et al.*, Nature (London) **439**, 45 (2006).

[5] M. Limongi and A. Chieffi, Astrophys. J. **647**, 483 (2006).

[6] C. Iliadis, A. Champagne, A. Chieffi, and M. Limongi, Astrophys. J., Suppl. Ser. **193**, 16 (2011).

[7] S. E. Woosley and A. Heger, Rev. Mod. Phys. **74**, 1015 (2002).

[8] A. Palacios *et al.*, Astron. Astrophys. **429**, 613 (2005).

[9] D. Vescovi *et al.*, Astrophys. J. Lett. **863**, 115 (2018).

[10] P. E. Koehler, R. W. Kavanagh, R. B. Vogelaar, Y. M. Gledenov, and Y. P. Popov, Phys. Rev. C **56**, 1138 (1997).

[11] H. P. Trautvetter, H. W. Becker, U. Heinemann, L. Buchmann, C. Rolfs, F. Käppeler, M. Baumann, H. Freiesleben, H. J. Lütke-Stetzkamp, P. Geltenbort, and F. Gönnewein, Z. für Physik A **323**, 1 (1986).

[12] B. M. Oginni, C. Iliadis, and A. E. Champagne, Phys. Rev. C **83**, 025802 (2011).

[13] S. Benamara, N. de Séréville, A. M. Laird, F. Hammache, I. Stefan, P. Roussel, S. Ancelin, M. Assié, A. Coc, I. Deloncle *et al.*, Phys. Rev. C **89**, 065805 (2014).

[14] L. De Smet, C. Wagemans, J. Wagemans, J. Heyse, and J. Van Gils, Phys. Rev. C **76**, 045804 (2007).

[15] C. Lederer-Woods (unpublished).

[16] C. Weiss *et al.* (n_TOF Collaboration), Nucl. Instrum. Methods Phys. Res., Sect. A **799**, 90 (2015).

[17] C. Ingelbrecht, A. Moens, J. Wagemans, B. Denecke, T. Altzitzoglou, and P. Johnston, Nucl. Instrum. Methods Phys. Res., Sect. A **480**, 114 (2002).

[18] A. D. Carlson *et al.*, Nucl. Data Sheets **148**, 143 (2018).

[19] M. Sabate-Gilarte *et al.* (n_TOF Collaboration), Eur. Phys. J. A **53**, 210 (2017).

[20] J. Wagemans, C. Wagemans, G. Goeminne, P. Geltenbort, A. Moens, Nucl. Phys. A **696**, 31 (2001).

[21] R. L. Macklin and J. H. Gibbons, Rev. Mod. Phys. **37**, 166 (1965).

[22] T. Rauscher and F. K. Thielemann, At. Data Nucl. Data Tables **79**, 47 (2001).

[23] R. H. Cyburt *et al.*, Astrophys. J., Suppl. Ser. **189**, 240 (2010).

[24] G. R. Caughlan and W. F. Fowler, At. Data Nucl. Data Tables **40**, 283 (1988).

[25] M. A. Van Raii *et al.*, Astron. Astrophys. **478**, 521 (2008).